Published by
NIGERIAN SOCIETY OF PHYSICAL SCIENCES
Available online @ https://journal.nsps.org.ng/index.php/jnsps

J. Nig. Soc. Phys. Sci. 6 (2024) 2011

Journal of the Nigerian Society of Physical Sciences

Sonochemical synthesis and characterization of Fe(II) and Cu(II) nano-sized complexes of sulfamethoxazole

B. C. Asogwa*, I. E. Otuokere

Department of Chemistry, Michael Okpara University of Agriculture Umudike, Abia State

Abstract

Nanoparticle drug delivery systems are precisely designed technologies that utilize nanoparticles to deliver therapeutic drugs to specific targets and regulate their release. In recent times, nanoparticles have garnered significant interest owing to their potential for efficient drug delivery. This work is aimed at synthesizing Fe(II) and Cu(II) nano-sized complexes of sulfamethoxazole (SMX) using the sonication method. The physical and spectroscopic studies showed a colour change from white to grey, and a decrease in melting points suggested the formation of the metal complexes. The nanometal complexes were insoluble in water. XRD analysis showed that the crystallite sizes of Fe(II) and Cu(II) nanometal complexes were determined to be 76.08 nm and 37.13 nm, respectively, using the Debye-Scherrer equation. The FTIR results of the SMX, Fe(II), and Cu(II) nanometal complexes showed a shift of the amine band from 3243 to 3191 cm^{-1} and the sulfone band from 1154 to 1092 cm^{-1} in both complexes. The proton NMR showed a shift of the amine proton from 6.100 ppm to 6.035 ppm in the spectra of the Cu(II) complex. The amine chemical shift was absent in the spectra of the Fe(II) complex, showing deprotonation. The carbon-13 NMR spectra showed a similar chemical shift. The spectra studies indicated that SMX coordinated with the metal ions through the amino and sulfone groups. A tetrahedral structure was proposed for the complexes. SMX coordinated as a bidentate ligand to Fe(II) and Cu(II) ions.

DOI:10.46481/jnsps.2024.2011

Keywords: Sulfamethaxazole, Nanometal, Complexes, FTIR, XRD, NMR

Article History :
Received: 12 February 2024
Received in revised form: 29 April 2024
Accepted for publication: 27 May 2024
Published: 19 June 2024

Communicated by: Emmanuel Etim

1. Introduction

Nanoparticles (NPs) are a formulation with a diameter below 100 nm [1]. NPs possess a size that is comparable to the dimensions of existing functional units. This enables engagement with nucleic acids, proteins, or lipids. Due to this characteristic, there has been a notable augmentation in the movement of nanoparticles into internal cellular structures when compared to bigger particles made of the same metals [2]. An exceptional benefit of nanoparticles is their capacity to infiltrate flawed blood capillaries, resulting in enhanced uptake of the encapsulated medication by infected cells in comparison to normal cells. Nanoparticles provide protection against drug inactivation and improve the drug substance's distribution qualities. Utilizing nanoparticles allows for the augmentation of physicochemical properties by greatly improving the compound's solubility. This leads to easier drug administration to patients and longer retention time in the human body [3].

The administration of structurally modified drugs, espe-

*Corresponding author Tel. No.: +234-706-292-8066.
Email address: chidonwasogwa@gmail.com (B. C. Asogwa)

cially metal complexes, has been shown to possess better toxicological and pharmacological properties [4, 5]. These improved properties, especially complexes, have been identified to show favorable biopharmaceutical activity pertinent to dosage formation and drug delivery [6, 7]. This became necessary because the continuous abuse (misuse) of antibiotics has caused a gross growth in the number of bacteria that are resistant to drugs [8, 9]. Researchers have observed that several transition metals, due to their ability to bind nucleophilic (electron- rich) components such as proteins and DNA, have various effects on biological processes [10, 11]. This discovery has also led to research into adding metal ions, especially transition metals, to the structure of of drugs so that they can interact with biological systems in a way that is controlled and has a healing effect [12, 13]. Transition metals tend to bond to a variety of molecules known as coordination compounds due to the presence of partially filled d-orbitals [12, 14].

The quest for the discovery and synthesis of more efficacious therapies, therapeutic materials, and other tools, as well as devices of lower toxicity than the existing ones, has led to the development of new nanomaterials, some of which have shown high biomedical performance [15]. The micromic size in addition to the large surface area of nanoparticles has become a reason for the enhanced colloidal stability, leading to an increase in the bioavailability score, which demonstrates the capacity to cross the blood-brain barrier, enter the pulmonary system, and absorb endothelial cells [16]. In recent times, scientists have faced the challenge of balancing the positive and therapeutic effects of metal oxide nanoparticles with their negative effects or toxicity, which has become a significant obstacle to the development of nanoparticles [15].

SMX (Figure 1) has been judged to be the most used sulfonamide in the area of human medicine for the reason that it is a good bacteriostatic antibiotic [17]. Its use is very prominent in synergistic combination therapy [18]. The discovery of sulfonamides came as an alternative to the hypersensitivity of penicillin because of its ability to interfere by reaction with p-aminobenzoic acid (PABA) during the synthesis of tetrahyfrofolic acid in biological systems, therefore influencing the bacterial metabolic process [19]. Several drugs containing sulfa compounds have been identified as treatments for malaria, leprosy, tuberculosis, and even cancer [20], but the incessant bacterial resistance to these drugs has in the past few years limited their use and also made for modified forms of these compounds for more therapeutic use. The field of medicinal inorganic chemistry has advanced as a result of the discovery that physiologically active molecules and metals combine to produce better therapeutic compounds [21]. The SMX molecule has donor atoms like nitrogen, oxygen, and sulphur in different parts of its structure. These enable it to behave as a polydentate ligand, connecting with different metal ions to form chelates [22].

Rostamizadeh *et al.* [23] reported the synthesis of SMX complexes, but to the best of our knowledge, the synthesis of Fe(II) and Cu(II) nano-sized complexes of SMX is yet to be reported. We hereby report the sonochemical synthesis and characterization of Fe(II) and Cu(II) nano-sized complexes of SMX for future biological activity.

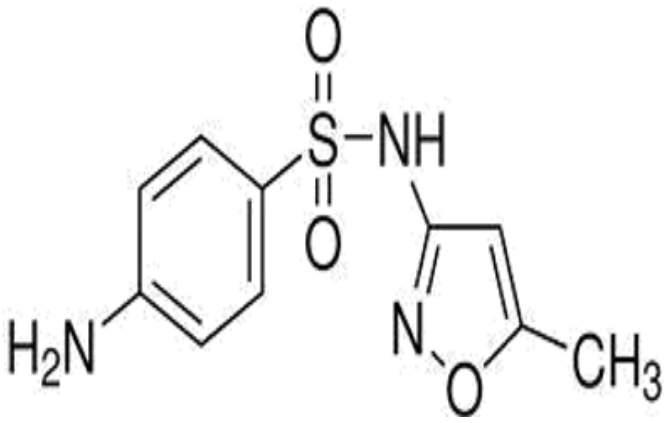

Figure 1. Chemical structure of sulfamethoxazole.

Table 1. Melting points of SMX and its nanometal complexes.

Compounds	Colour	MP (°C)	% Yield
SMX	white	172	-
$[Fe(SMX)(H_2O)_2]$	grey	150	75
$[Cu(SMX)(H_2O)_2]$	grey	160	81

2. Materials and Methods

2.1. Chemicals and solvents

The analytical grade SMX salt was obtained from Andhra Organics Limited, India.

2.2. Synthesis of Fe (II) and Cu (II) nano-sized of SMX by ultrasonic sonicator method

The nanometal complexes were synthesized *by ultrasonic sonicator method* described by Abdel- Rahman *et al.* [24]. Equimolar (0.1 mole) solutions of SMX (2.53 g) and metal ions (2.78 g of FeSO4.7H2O and 1.59 g of CuSO4.5H2O) each were added together. The mixture was stirred and positioned on an ultrasonic probe of an ultrasonic sonicator that operates at 24 kHz with a maximum force output of 400 W for 30 minutes. The mixture obtained was filtered with a Whatman No. 1. filter paper. The filtrates were then carefully kept in the desiccator to dry. Each of the complexes was stored in a neatly labeled container.

2.3. Physical and spectroscopic analysis

2.3.1. Melting Point

The melting points (in degrees) for the nanometal complexes were carried out using the Gallenkamp melting point apparatus.

2.3.2. Solubility Test

The solubility of SMX and nanometal complexes was tested using different solvents of varied polarity, such as n-hexane, ethanol, water, ethyl acetate, and dimethylsulfoxide. Exactly 0.1g of the complex was taken and dissolved into a corresponding 3 ml of the solvents at 25 °C.

Table 2. Solubility profile of SMX and its nano metal complexes.

Compounds	n-Hexane	Distilled water	Ethanol	Ethyl Acetate	DMSO
SMX	SS	SS	S	S	S
$[Fe(SMX)(H_2O)_2]$	SS	IS	S	S	S
$[Cu(SMX)(H_2O)_2]$	SS	IS	S	S	S

Table 3. Summary of the UV/vis peaks; a comparism of the SMX and its nano metal complexes.

Compounds	Transitions	λmax (nm)
SMX	$\pi \rightarrow \pi*$	302, 306, 311, 316, 320, 325
$[Fe(SMX)(H_2O)_2]$	$\pi \rightarrow \pi*$	209
	$n \rightarrow \pi*$	269
	$^5T_{2g} \rightarrow {}^5E_g$	548
$[Cu(SMX)(H_2O)_2]$	$\pi \rightarrow \pi*$	209
	$n \rightarrow \pi*$	269

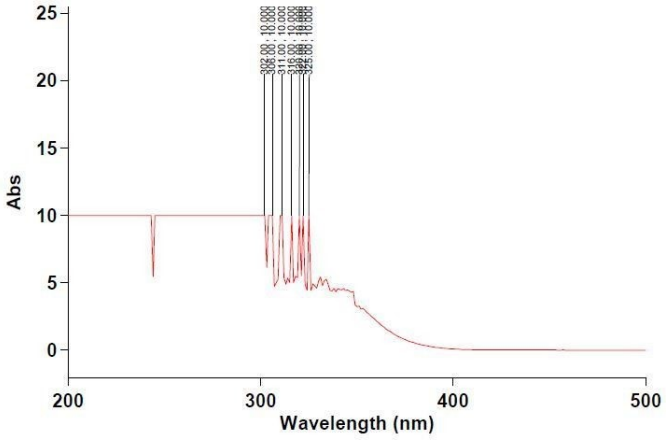

Figure 2. UV/Visible spectrum of SMX.

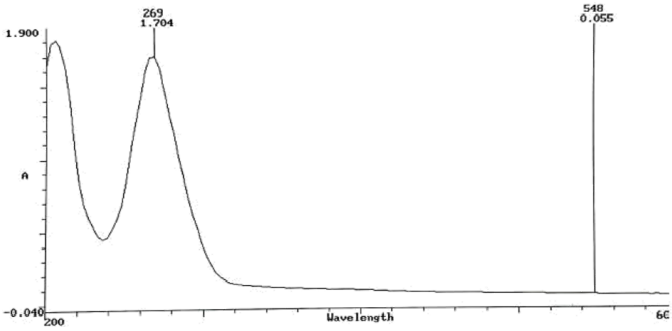

Figure 3. UV/Visible spectrum of $[Fe(SMX)(H_2O)_2]$.

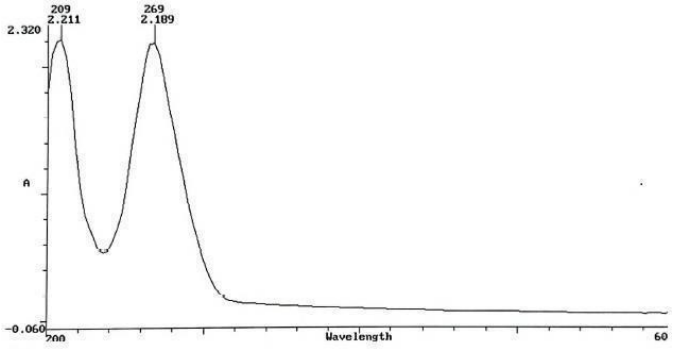

Figure 4. UV/Visible spectrum of $[Cu(SMX)(H_2O)_2]$.

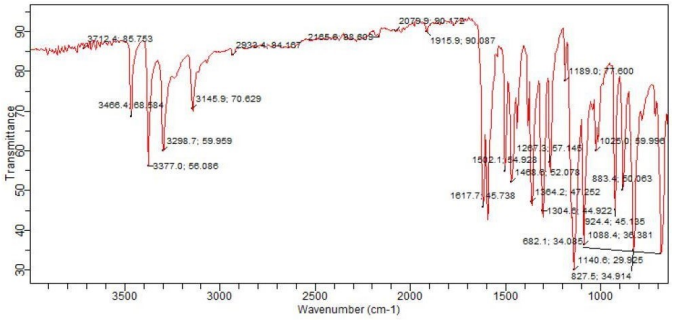

Figure 5. FTIR spectrum of SMX.

2.3.3. *UV/Visible spectroscopy*

The UV/Visible spectral measurements of the synthesized nanometal complexes were obtained using a UV-1800 series using dimethoxysulfoxide as solvent.

2.3.4. *Infrared spectroscopy*

The ligand and nanometal complexes were subjected to FT-IR spectra analysis. IR spectra were obtained using a Perkin Elmer Spectrum BX FT-IR spectrophotometer (4400–600 cm^{-1}) in KBr pellets.

2.3.5. *Characterization of the nano-sized particles by x-ray diffraction*

The pulverized samples were pelletized, sieved to 0.074 mm, and then taken with an aluminium alloy grid (35mm x 50mm) on a flat glass plate and covered with paper. Wearing hand gloves, the samples were gently pressed with the hand to become compact and ran through the Rigaku D/Max-lllC X-ray diffractometer. The machine was set to produce diffractions at a scanning rate of 2.0/min in the range of 2 to 500 at room temperature with CuKa radiation set at 40 kV and 20 mA. The crystallite size of the nanometal complexes was calculated us-

Table 4. Summary of the IR peaks; a comparison of SMX and its complexes.

	Absorption bands in cm^{-1}				
Compounds	N-H	S=O	C-O	M-N	M-O
SMX	3299	1305, 1140	1267	-	-
$[Fe(SMX)(H_2O)_2]$	3243	1308, 1092	1267	757	667
$[Cu(SMX)(H_2O)_2]$	3191	1304, 1092	1267	783	671

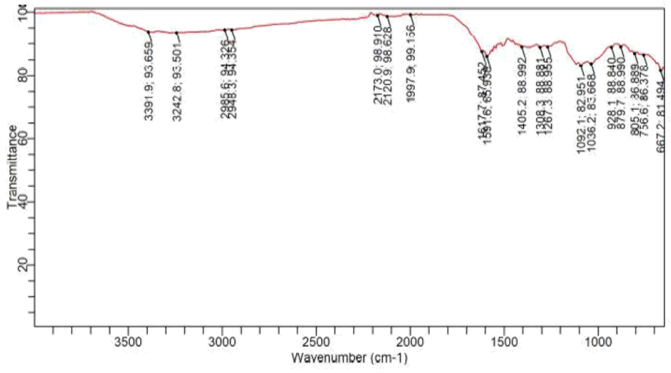

Figure 6. FTIR spectrum of [Fe(SMX)(H2O)2].

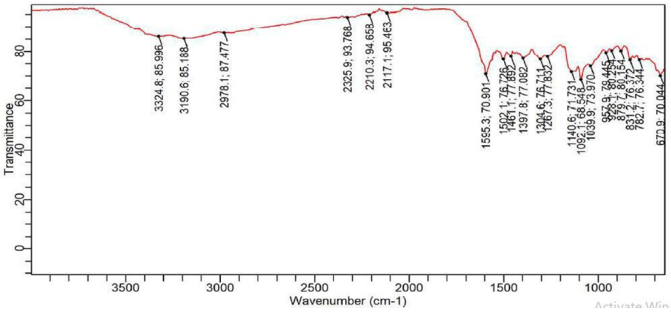

Figure 7. FTIR spectrum of $[Cu(SMX)(H_2O)_2]$.

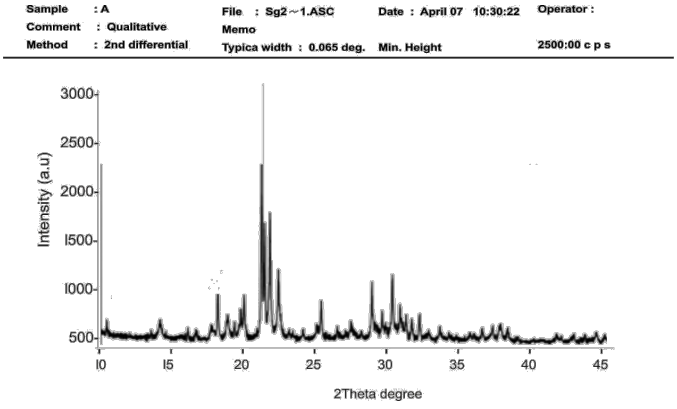

Figure 8. XRD pattern of $[Fe(SMX)(H_2O)_2]$.

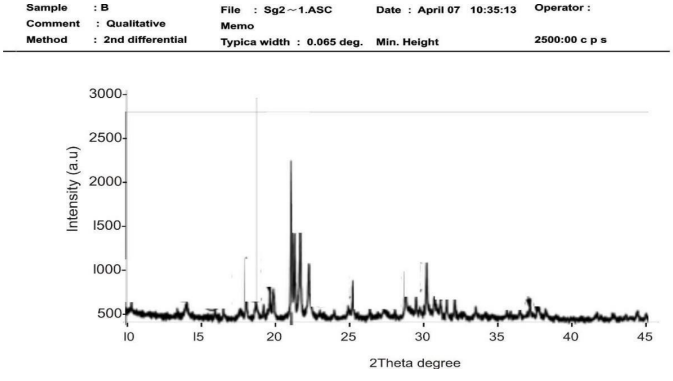

Figure 9. XRD pattern of $[Cu(SMX)(H_2O)_2]$.

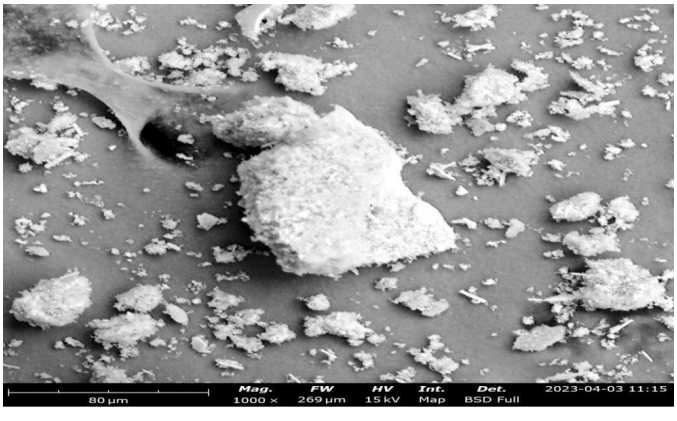

Figure 10. SEM monograph of $[Fe(SMX)(H_2O)_2]$.

ing Debye-Scherrer's equation, D=Kλ/ (β cos θ) where D is the crystallite size of nanoparticles, K is the Scherrer constant = 0.98, λ is wavelength. β is the full width at half maximum (FWHM).

2.3.6. Nuclear magnetic resonance

The NMR spectra measurements were obtained on a Nanalysis X-685 benchtop NMR with a machine frequency of 60 MHz and using deuterated DMSO as solvent.

3. Results and Discussion

3.1. Colour, Melting point and yield (%)

The colour, melting point and yield (%) are presented in Table 1.

SMX and their metal complexes are crystalline, non-hygroscopic, and air-stable compounds. The change in colour from white (ligands) to grey suggested that coordination occurred as transition metal complexes are coloured [25, 26]. The nanometal complexes of SMX were observed to have melting points lower than those of the ligand. This could be attributed to an increased proportion of surface atoms as the size of particles decreases [27].

Table 5. The XRD spectra data showing the 2θ, FWHM, wavelength and particle size.

Compound	2θ,	FWHM	λ (Å)	Crystallite size (nm)
$[Fe(SMX)(H_2O)_2]$	25.515	0.12	1.654	76.08
$[Cu(SMX)(H_2O)_2]$	34.345	0.238	1.568	37.13

Table 6. Summary of the ^{1}H NMR bands; a comparison of the ligand SMX and its complexes.

	Chemical shift in ppm			
Compounds	H of Isoxazole	H of aromatic	H of methyl	H of H_2O
SMX	6.107	6.598, 7.485	2.290	-
$[Fe(SMX)(H_2O)_2]$	5.995	6.528, 7.397	2.471	3.375
$[Cu(SMX)(H_2O)_2]$	6.035	6.635, 7.360	2.295	3.312

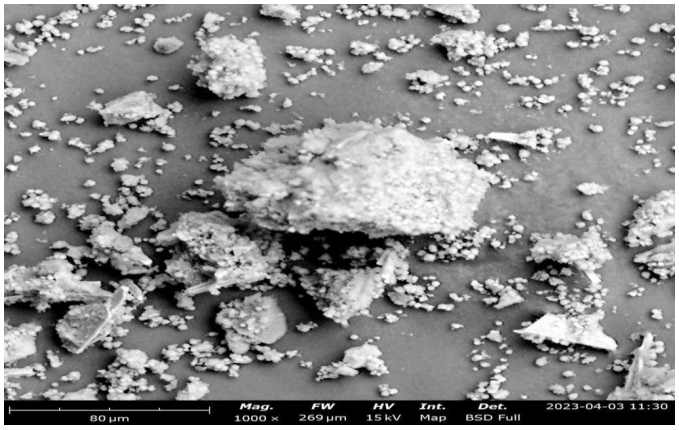

Figure 11. SEM monograph of $[Cu(SMX)(H_2O)_2]$.

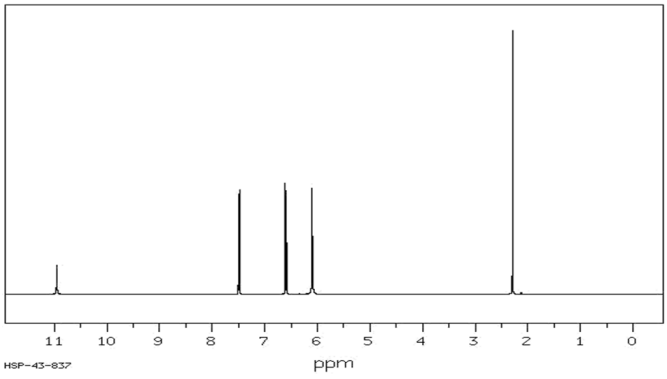

Figure 12. ^{1}H spectrum of SMX (source: spectra database for organic compounds SDBS).

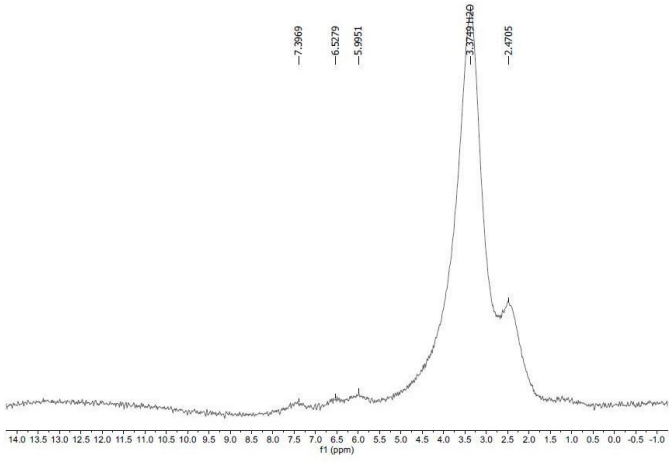

Figure 13. ^{1}H spectrum of $[Fe(SMX)(H_2O)_2]$.

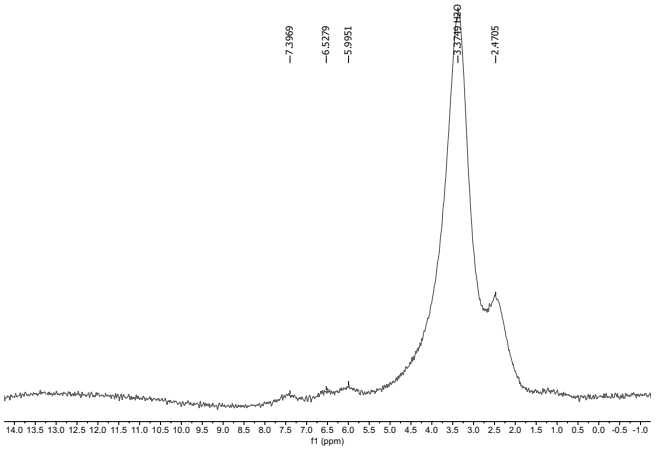

Figure 14. ^{1}H spectrum of $[Fe(SMX)(H_2O)_2]$.

3.2. *Solubility*

The solubility profile of SMX and its nanometal complexes are presented in Table 2.

SMX, Fe(II), and Cu(II) nanometal complexes were all soluble in ethyl acetate and DMSO because DMSO and ethylacetate are both known to be polar aprotic solvents as they dissolve both non-polar and polar compounds as well as being miscible in different organic solvents [28].The SMX was slightly soluble in distilled water, while the nanometal complexes were insoluble. The insolubility of the complexes in water could be attributed to a decrease in polarity.

3.3. *UV/Visible spectroscopy*

The summary of the UV/visible spectral data is presented in Table 3, while the spectra are shown in Figures 2, 3, and 4.

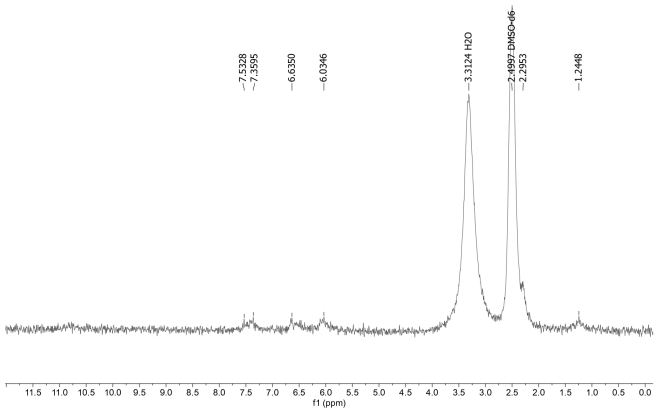

Figure 15. ^{1}H spectrum of [Cu(SMX)$(H_2O)_2$].

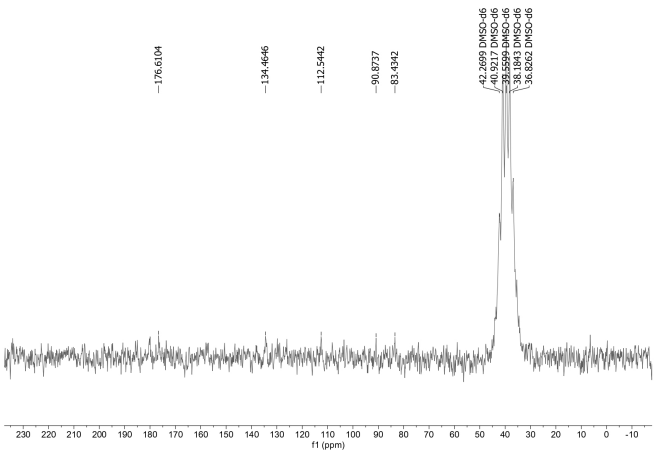

Figure 17. ^{13}C NMR spectrum of [Fe(SMX)$(H_2O)_2$].

Table 7. Summary of the ^{13}C NMR bands; a comparison of the SMX and its complexes.

Compounds	Some chemical shift in ppm	
	C=N	C-O
SMX	157.86	169.79
[Fe(SMX)$(H_2O)_2$]	151.46	176.61
[Cu(SMX)$(H_2O)_2$]	160 .68	169.36

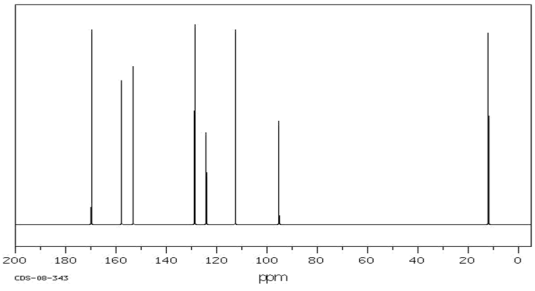

Figure 16. ^{13}C NMR spectrum of SMX (source: spectra database for organic compounds SDBS).

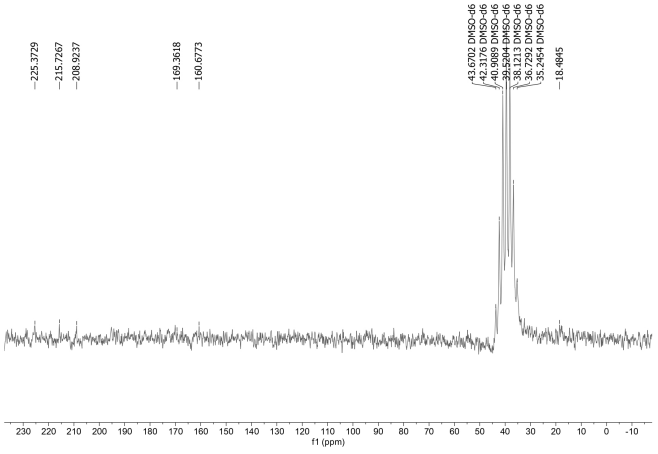

Figure 18. ^{13}C NMR spectrum of [Cu(SMX)$(H_2O)_2$].

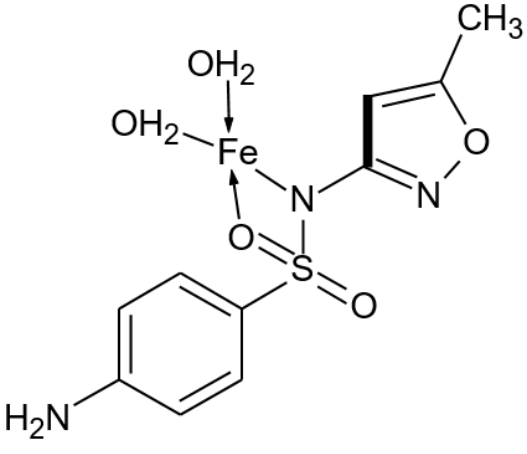

Figure 19. Proposed structure for [Fe(SMX)$(H_2O)_2$].

The transitions at λ = 209 and 269 nm in the nanometal complexes were assigned to the $\pi \rightarrow \pi*$ and n $\rightarrow \pi*$. These transitions are known as inter-ligand charge transfer (ILCT) [29]. The absorption band at λ = 548 nm observed for the [Fe(SMX)$(H_2O)_2$] metal complex has been assigned d-d transitions since it was a weak transition [30].

3.4. Infrared Spectroscopy

Summary of the IR peaks are shown in Table 4. The spectra are presented in Figures 5, 6 and 7.

A strong band at 3299 cm^{-1} which was exhibited by SMX, was assigned to NH_2. This band was shifted to 3243 cm^{-1} and 3191 cm^{-1} in the spectra of [Fe(SMX)$(H_2O)_2$] and [Cu(SMX)$(H_2O)_2$] nanometal complexes, respectively, showing that the nitrogen of the amino group is coordinated to the metal ions without deprotonation [31]. The sulfone band at 1305 cm^{-1} in SMX remained unchanged (1308 cm^{-1} and 1304 cm^{-1}) in [Fe(SMX)$(H_2O)_2$] and [Cu(SMX)$(H_2O)_2$] respectively, while the second sulfone band at 1154 cm^{-1} in SMX shifted to 1092 cm^{-1} in the metal complexes, showing a coordination of SMX to the metal ion through the sec-

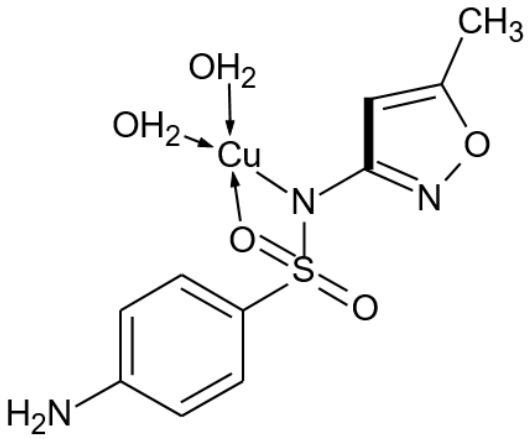

Figure 20. Proposed structure for $[Cu(SMX)(H_2O)_2]$.

ond sulfone oxygen atom. Bamigboye et al. [32] reported a similar shift. The bands for (M-N) and (M-O) were observed within the range of 783–757 cm^{-1} and 671–667 – 667 cm^{-1}, respectively, in the spectra of the nanometal complexes. These bands were absent in the SMX spectra, further confirming the coordination of NH_2 and S=O. was shifted to 3243 cm^{-1} and 3191 cm^{-1} in the spectra of $[Fe(SMX)(H_2O)_2]$ and $[Cu(SMX)(H_2O)_2]$ nanometal complexes, respectively, showing that the nitrogen of the amino group is coordinated to the metal ions without deprotonation [31]. The sulfone band at 1305 cm^{-1} in SMX remained unchanged (1308 cm^{-1} and 1304 cm^{-1}) in $[Fe(SMX)(H_2O)_2]$ and $[Cu(SMX)(H_2O)_2]$ respectively, while the second sulfone band at 1154 cm^{-1} in SMX shifted to 1092 cm^{-1} in the metal complexes, showing a coordination of SMX to the metal ion through the second sulfone oxygen atom. Bamigboye *et al.* [32] reported a similar shift. The bands for (M-N) and (M-O) were observed within the range of 783–757 cm^{-1} and 671–667 – 667 cm^{-1}, respectively, in the spectra of the nanometal complexes. These bands were absent in the SMX spectra, further confirming the coordination of NH_2 and S=O.

3.5. XRD

The XRD spectra data is presented in Table 5, while the diffraction patterns are presented in Figures 8 and 9.

The XRD pattern showed that the Fe(II) and Cu(II) nanocomplexes are crystalline. Using the Debye- Scherrer's equation, $D=K\lambda/(\beta \cos \theta)$, the crystallite sizes of the nanocomplexes were calculated. The crystallite sizes of Fe(II) and Cu(II) nanocomplexes were 76.08 and 37.13 nm, respectively.

3.6. SEM

The micrographs in this study revealed that $[Fe(SMX)(H_2O)_2]$ and $[Cu(SMX)(H_2O)_2]$ nanoparticles are seen to be rough and irregular shaped with some pore spaces, which gives an idea that the nanometal complexes of sulfamethoxazole could be a good inhibitor against clinical microorganisms.

3.7. NMR

The ^1H NMR spectral data are depicted in Table 6. The spectra are shown in Figures 12, 14 and 15.

The ^{13}C NMR spectral data are depicted in Table 7. The spectra are shown in Figures 16, 17 and 18.

The obtained ^1H NMR spectrum of SMX was seen to have exhibited a peak at 6.107 ppm, corresponding to the proton of isoxazole. This peak was observed at 5.995 and 6.035 ppm in $[Fe(SMX)(H_2O)_2]$ and $[Cu(SMX)(H_2O)_2]$, respectively. A chemical shift observed at 6.100 ppm was assigned to NH_2 in SMX. This signal was absent in the spectra of $[Fe(SMX)(H_2O)_2]$ due to deprotonation, while in $[Cu(SMX)(H_2O)_2]$, shifted to 6.035 ppm, showing coordination with metal through the nitrogen atom. A new peak that was absent in the spectrum of the ligand was observed at 3.375 and 3.312 ppm in the $[Fe(SMX)(H_2O)_2]$ and $[Cu(SMX)(H_2O)_2]$ complexes, respectively. This peak was assigned to the proton of a water molecule.

A comparison of the ^{13}C spectra of SMX and its nanometal complexes showed no significant chemical shift was observed with C=N and C=O bonds.

Based on the spectroscopic study, the proposed structures in Figures 19 and 20 have been proposed for the $[Fe(SMX)(H_2O)_2]$ and $[Cu(SMX)(H_2O)_2]$ nanocomplexes.

4. Conclusion

Synthesis and characterization of Fe(II) and Cu(II) nanocomplexes of SMX were carried out. The nanometal complexes were synthesized using the sonication method and characterized based on the observed FTIR spectra, electronic spectra, melting point, solubility, proton, and carbon-13 nuclear magnetic resonance. The XRD pattern showed that the Fe(II) and Cu(II) nanocomplexes are crystalline, having a crystallite size of 76.08 and 37.13 nm, respectively. A tetrahedral structure was proposed for the complex, which showed that SMX behaved as a bidentate ligand towards Fe (II) and Cu (II) ions.

References

[1] X. Chen, H. Li, X. Qiao, T. Jiang, X. Fu, Y. He & X. Zhao, "Agarose oligosaccharide- silver nanoparticle- antimicrobial peptidecomposite for wound dressing", Carbohydrate Polymer **269** (2021) 118258. https://www.sciencedirect.com/science/article/abs/pii/S0144861721006457.

[2] M. J. Khan, A. Ahmad, M. A. Khan & S. Siddiqui, "Zinc Oxide Nanoparticle Induces Apoptosis in Human Epidermoid Carcinoma Cells Through Reactive Oxygen Species and DNA Degradation", Biological Trace Element Research **199** (2021) 2172. https://link.springer.com/article/10.1007/s12011-020-02323-4.

[3] P. Redruello, G. Perazzoli, A. Cepero, F. Quiñonero, C. Mesas, K. Doello, A. Láinez-Ramos- Bossini, M. Rivera-Izquierdo, C. Melguizo & J. Prados, "Nanomedicine in Pancreatic Cancer: A New Hope for Treatment", Current Drug Targets **21** (2020) 580. https://doi.org/10.2174/1389450121666200703195229.

[4] I. E. Otuokere, J. C. Anyanwu, & K. K. Igwe, "Synthesis, Characterization and Antibacterial Studies of 4-{[(E)- Phenylmethylidene] amino}-N-(1,3-thiazol-2- yl)benzenesulfonamide and its Mn(II) Complex", Chemsearch Journal **11** (2020) 44. https://www.ajol.info/index.php/csj/article/view/197378.

[5] I. E. Otuokere, J. G. Ohwimu, K. C. Amadi, C. O. Alisa, F. C. Nwadire, O. U. Igwe, A. A. Okoyeagu & C. M. Ngwu. "Synthesis, characterization and molecular docking studies of Mn (II) complex of sulfathiazole", Journal of the Nigerian Society of Physical Sciences **1** (2019) 95. https://journal.nsps.org.ng/index.php/jnsps/article/view/20.

[6] I. E. Otuokere, D. O. Okorie, B. C. Asogwa, O. K. Amadi, L. O. C Ubani & F. C. Nwadire, "Spectroscopic and Coordination Behavior of Ascorbic Acid Towards Copper (II) Ion", Research in Analytical and Bioanalytical Chemistry **1** (2017) 1. https://www.academia.edu/35242668/Spectroscopic_and_Coordination_Behavior_of_Ascorbic_Acid_Towards_Copper_II_Ion.

[7] V. V. Shalygina, E. N. Vlasova & E. P. Anan'eva, "Synthesis, Physicochemical Properties, and Antimicrobial Activity of Polymyxin B1 Conjugates with Polyglutaraldehyde", Pharmceutical Chemistry Journal **53** (2019) 134. https://doi.org/10.1007/s11094-019-01967-4.

[8] H. Sirajul, S. Dildar, M. B. Ali, A. Mezni, A. Hedfi, M. I. Shahzad, N. Shahzad & A. Shah, "Antimicrobial and antioxidant properties of biosynthesized of NiO nanoparticles using *Raphanus sativus* (R. sativus) extract", Journal of Inorganic and Organometallic Polymers and Materials **31** (2020) 1134. https://iopscience.iop.org/article/10.1088/2053-1591/abfc7c/meta.

[9] I. O. Edozie, O. J. Godday, A. K. Chijioke, I. O. Uchenna, & N. F. Chigozie, "Synthesis, characterization and molecular docking studies of Co (II) metal complex of sulfathiazole", Bulletin of the Chemical Society of Ethiopia **34** (2020) 83. https://dx.doi.org/10.4314/bcse.v34i1.8.

[10] I. E. Otuokere, U. F. Robert & K. K. Igwe, "Chelating and Antibacterial Potentials of Benzylpenicillin and its Ni (II) Complex", Communication in Physical Sciences **8** (2022) 138. https://journalcps.com/index.php/volumes/article/view/269.

[11] I. E. Otuokere, U. F. Robert, K. K. Igwe & S. U. Mpama, "Synthesis, Characterization and Antibacterial Studies of Benzylpenicillin and its Co(II) Complex", ChemSearch Journal **11** (2020) 9. https://www.ajol.info/index.php/csj/article/view/197367.

[12] I. E. Otuokere, K. C. Nwaiwu, F. C. Nwadire, and O. U. Akoh, "Synthesis and characterization of Cr (III)-ascorbic acid complex" Journal of Applied Sciences and Environmental Management **26** (2022) 75. https://dx.doi.org/10.4314/jasem.v26i1.12.

[13] N. V. Loginova, H. I. Harbatsevich, N. P. Osipovich, G. A. Ksendzova, T. V. Koval'chuk & G. I Polozov, "Metal Complexes as Promising Agents for Biomedical Applications", Current Medicinal Chemistry **27** (2020) 5213. https://doi.org/10.2174/0929867326666190417143533.

[14] I. E. Otuokere, L. O. Okpara, K. C. Amadi, N. Ikpo, G. U. Okafor & F. C. Nwadire, "Synthesis, Characterization And Complexation Of Cr(III) Ion Using Chloroquine Diphosphate Drug", Journal of Chemical Society of Nigeria **44** (2019) 107. https://nijophasr.net/index.php/nijophasr/article/view/274.

[15] M. P. Nikolova, & M. S. Chavali, "Metal oxide nanoparticles and their applications in nanotechnology", SN Applied Resources **1** (2020) 607. https://link.springer.com/article/10.1007/s42452-019-0592-3.

[16] H. Chou-Yi , M. R. Ahmed, M. K. Mustafa, N. A. Nada, H. M. Srwa, H. A. Fatima, T. A. Zainab, M. A. Zahra, S. A. Zainab, K. H. Safa, K. A. Farah, H. M Zaid & K. Ehsan, " An overview of nanoparticles in drug delivery: Properties and applications", South African Journal of Chemical Engineering **46** (2023) 233. https://doi.org/10.1016/j.sajce.2023.08.009.

[17] G. Prasannamedha & P. S. Kumar, "A review on contamination and removal of sulfamethoxazole from aqueous solution using cleaner techniques: Present and future perspective", Journal of Cleaner Production **250** (2020) 119553. https://doi.org/10.1016/j.jclepro.2019.119553.

[18] J. S. Geraldine, N. N. Delgado, R. Maharjan & A. K. Cain, "How antibiotics work together: molecular mechanisms behind combination therapy", Current Opinion in Microbiology **57** (2020) 31. https://doi.org/10.1016/j.mib.2020.05.012.

[19] A. Ovung & J. Bhattacharyya, "Sulfonamide drugs: structure, antibacterial property, toxicity, and biophysical interactions", Biophysical Reviews **13** (2021) 259. https://link.springer.com/article/10.1007/s12551-021-00795-9.

[20] J. L. Siqueira-Neto, K. J. Wicht, K. Chibale, J. N. Burrows, D. A. Fidock & E. A. Winzeler, "Antimalarial drug discovery: progress and approaches", Nat Rev Drug Discovery **22** (2023) 807. https://doi.org/10.1038/s41573-023-00772-9.

[21] M. Samsonowicz, M. Kalinowska & K. Gryko, "Enhanced antioxidant activity of Ursolic acid by complexation with Copper (II): experimental and theoretical study", Materials **14** (2021) 264. https://doi.org/10.3390/ma14020264.

[22] M. M. Abdul-Hassan & N. K. Mousa, *Antimicrobial activity of new transition metal complexes of sulfamethoxazole on nhibiter by Staphylococcus aureus, Pseudomonas aeruginosa, Salmonella typhi and Escherichia coli*, In AIP Conference Proceedings, 2020, AIP Publishing, 2290. https://pubs.aip.org/aip/acp/article/2290/1/030037/1001400/Antimicrobial-activity-of-new-transition-metal.

[23] S. Rostamizadeh, Z. Daneshfar & H. Moghimi, "Synthesis of sulfamethoxazole and sulfabenzamide metal complexes; evaluation of their antibacterial activity", European Journal of Medicinal Chemistry **171** (2019) 364. https://doi.org/10.1016/j.ejmech.2019.03.002.

[24] N. Zare, A. Zabardasti, A. Mohammadi, "Sonochemical synthesis, characterization, biological applications, and DFT study of new nano-sized manganese complex of azomethine derivative of diaminomaleonitrile", Journal of Iran Chemical Society **16** (2019) 1501. https://doi.org/10.1007/s13738-019-01626-1.

[25] O. Ugochukwu & I. E. Otuokere, "Synthesis, Spectroscopic Characterization and Antibactrial Activities of Co (II) Complex of Ofloxacin Drug Mixed with Ascorbic Acid as a Secondary Ligand", BioScientific Review **3** (2021) 1. https://doi.org/10.32350/BSR.0303.01.

[26] S. J. Almehmadi, A. Alharbi, M. M. Abualnaja, K. Alkhamis, M. Alhasani, S. H. Abdel-Hafez, R. Zaky & N. M. El-Metwaly, "Solvent free synthesis, characterization, DFT, cyclic voltammetry and biological assay of Cu(II), Hg(II) and UO_2(II) – Schiff base complexes", Arabian Journal of Chemistry **15** (2022) 103586. https://doi.org/10.1016/j.arabjc.2021.103586.

[27] A. Al-Rsheed, S. Aldawood & O. Aldossary, "The Size and Shape Effects on the Melting Point of Nanoparticles Based on the Lennard-Jones Potential Function", Nanomaterials (Basel) **30** (2021) 2916. https://www.mdpi.com/2079-4991/11/11/2916.

[28] S. Sarala, S. K. Geetha, S. Muthu & A. Irfan, "Theoretical investigation on influence of protic and aprotic solvents effect and structural (Monomer, Dimer), Van-der Waals and Hirshfeld surface analysis for clonidine molecule", Computational and Theoretical Chemistry **1204** (2021) 113397. https://doi.org/10.1016/j.comptc.2021.113397.

[29] M. H. Gençkal, M. Erkisa, P. Alper, S. Sahin, E. Ulukaya & F. Ari, "Mixed ligand complexes of Co(II), Ni(II) and Cu(II) with quercetin and diimine ligands: synthesis, characterization, anti-cancer and antioxidant activity", Journal of Biological Inorganic Chemistry **25** (2020) 161. https://doi.org/10.1007/s00775-019-01749-z.

[30] I. E. Otuokere & U. F. Robert, "Synthesis, Characterization and Antibacterial Studies of (3, 3- Dimethyl-7-oxo-6-(2-phenylacetamido)-4-thia-1-azabicyclo [3.2. 0]heptane-2-carboxylic acid-Cr (III) Complex", Journal of Nepal Chemical Society **41** (2020) 1. https://doi.org/10.3126/jncs.v41i1.30370.

[31] A. Kotynia, B. Wiatrak, W. Kamysz, D. Neubauer, P. Jawień & A. Marciniak, "Cationic Peptides and their Cu(II) and Ni(II) Complexes: Coordination and Biological Characteristics", International Journal of Molecular Science **22** (2021) 12028. https://doi.org/10.3390/ijms222112028.

[32] M. O. Bamigboye, J. A. Obaleye & S. Abdulmolib, "Synthesis, characterization and antimicrobial activity of some mixed Sulfamethoxazole-cloxacillin metal drug complexes", International Journal of Chemistry **22** (2012) 105. https://www.researchgate.net/publication/275039892_Synthesis_Characterization_and_Antimicrobial_Activity_of_Some_Mixed_Trimethoprim_-Sulfamethoxazole_Metal_Drug_Complexes.